Magnetic properties of the dipolar Heisenberg antiferromagnet Gd in $GdBa_2Cu_3O_{6+x}$

K. Nehrke and M.W. Pieper
Institut für Angewandte Physik, Universität Hamburg, Jungiusstraße 11, D-20355 Hamburg, Germany
(Received 6 December 1994)

The nuclear spin-lattice and spin-spin relaxation times (T_1, T_2) and the rf enhancement factor η of ^{63,65}Cu in $GdBa_2Cu_3O_{6+x}$ were investigated at low temperatures (1.3–4.2 K) and in magnetic fields up to 7 T. T_1 and T_2 of the Cu(1) and Cu(2) sites were measured in the whole temperature range for various oxygen concentrations. The phase transition of the Gd sublattice is well resolved with $T_N = 2.19$ K for $x = 0$, decreasing slightly to $T_N = 2.09$ K for $x = 1$. The temperature dependence of the Gd fluctuations is in good agreement with the two-dimensional (2D) Ising model, indicating a breaking of the expected Heisenberg symmetry for the $^8S_{7/2}$ Gd spins by a uniaxial anisotropy. We propose that this is due to the dipolar interaction, similar to the behavior observed in the classical 2D dipolar Heisenberg antiferromagnets of the K_2MnF_4 family. The critical field was determined for the semiconducting samples as a function of temperature by a maximum in T_2^{-1}. Extrapolation of the critical field to $T = 0$ yields $\mu_0 H_c(T = 0) = 3.1$ T. Enhancement factors up to $\eta = 15$ were observed at the spin-flop field $\mu_0 H_{sf} = 0.6$ T in the nonsuperconducting samples. From the spin-flop and the critical field we find an in-plane exchange $J/k_B \approx 75$ mK and an anisotropy field $\mu_0 H_a = 0.1$ T, which is in accord with the dipolar anisotropy calculated for the Gd sublattice.

I. INTRODUCTION

A short time after the discovery of high-T_c superconductivity in $YBa_2Cu_3O_{6+x}$ it was noticed that Y could be replaced by nearly all rare earth (RE) elements without influence on the transition temperature. This indicates that the magnetic RE moments and the superconducting hole bands in the adjacent CuO planes are well separated in the layered structure. Since this decoupling has been established experimentally and theoretically, there is a growing interest in the question of the coupling mechanisms along the c axis within the superconducting CuO and magnetic RE sublattice, respectively. The magnetic RE layers represent an isostructural series suitable for the study of crystalline-field effects and dipolar interactions.[1] An obvious aim of these investigations is to utilize the RE magnetism in the future as a probe for the magnetic and superconducting properties of the adjacent CuO planes.

The magnetic properties of Gd in this series are of special interest because of two reasons. First the Néel temperature of $T_N = 2.2$ K is more than 1 K higher than for the other rare earths.[2] Only Pr, which destroys superconductivity in the CuO layers, shows a markedly higher transition temperature ($T_N \approx 17$ K).[3] Second the magnetism of the Gd is simpler than for the other RE's, since crystalline-field effects are negligible for the $^8S_{7/2}$ state of Gd. The dipolar interaction cannot be neglected, it is in the order of the thermal energy at T_N. Differences in the dipolar energies of the Gd sublattice up to 3 K have been calculated.[4] For the large magnetic moments a Heisenberg exchange and the dipolar interaction should therefore be sufficient for the analysis of the Gd magnetism.

The Néel temperature is well established by neutron diffraction, specific heat, magnetic susceptibility, and Mössbauer spectroscopy[5–8] and depends only slightly on the oxygen concentration x. The results from neutron diffraction of Mook *et al.* and Mössbauer spectroscopy of Bornemann *et al.* showed that the Gd moments are aligned along the c axis.[5,9] The order is antiferromagnetic in the a-b plane but along the c axis ferromagnetic as well as antiferromagnetic arrangements were reported,[5,10] indicating a comparably weak coupling in this direction. It is interesting to note that the coupling between the Gd planes might depend on the presence of Al on the Cu(1) sites,[11] which also influences the stacking of the antiferromagnetic CuO layers for small oxygen concentrations.[12] From low temperature magnetization measurements Oguro *et al.* find a critical field of $\mu_0 H_c \approx 3.0$ T.[13] Meyer *et al.* give an estimate of $\mu_0 H_{sf} \approx 0.5$ T for the spin-flop field.[8] These values are consistent with the exchange field 0.9 T determined by Nakamura *et al.* from electron-spin resonance.[14]

From the layered structure two-dimensional (2D) dipolar Heisenberg behavior is expected. The experimental situation is somewhat controversial. Evidence for 2D behavior was reported from low frequency fluctuations present in the Gd-Mössbauer spectrum well below T_N and from the temperature dependence of the susceptibility.[8] Niedermayer *et al.* also detected very low frequency fluctuations with μSR at a temperature more than an order of magnitude above T_N.[15] This is in contrast to the result of Mook *et al.*, who reported only long range 3D coupling without significant 2D critical scattering in neutron diffraction.[5] Most of the studies of the Gd magnetism up to now were in zero field or used powder or ceramic samples, where the key parameters like critical and spin-flop fields are difficult to determine. Nuclear

magnetic resonance (NMR) as a local probe is sensitive to anisotropies to some degree even for powder samples. This allows a more detailed study of the magnetic phase diagram of the Gd sublattice in the absence of large, homogeneous and Al-free crystals.

The Gd hyperfine field in the ordered state is known from Mössbauer-spectroscopy,[8] but no ^{155,157}Gd resonance is observed at the corresponding NMR frequency ($\approx$ 50 MHz). This is most probably due to a fast relaxation of the nuclear spins induced by the strong fluctuations of the Gd moments observed in the Mössbauer spectrum. The Cu quadrupole resonance (NQR) of the plane and chain sites and the zero-field NMR of the Cu planes (at small x) of $GdBa_2Cu_3O_{6+x}$ is well known from numerous studies. It has been investigated in detail at low temperatures to clarify the oxygen coordination corresponding to the different Cu lines and to study the oxygen ordering in the Cu chains.[16] We therefore conducted detailed measurements of the spin-lattice and spin-spin-relaxation times (T_1, T_2) at the Cu-chain [Cu(1)] and Cu-plane sites [Cu(2)]. In this work we extend our recent investigations of the nuclear relaxation times[17] and present for the first time our results on the Cu enhancement factor.

II. EXPERIMENTAL PROCEDURE

The same powder samples with oxygen concentrations from $x = 0$ (empty CuO chains) to $x = 1$ (filled CuO chains) which Heinmaa *et al.* studied to identify the Cu lines of the various oxygen coordinations in $GdBa_2Cu_3O_{6+x}$,[16] were investigated in this work at low temperatures and in external fields. The oxygen concentration has been determined during preparation from a gravimetric analysis during the oxydization of carefully degassed samples[18] and was consistent with the NMR spectra of Heinmaa *et al.* The linewidth of the Cu(1)-site resonance for $x = 0$ is $\Delta f \approx 300$ kHz. This is only a factor of 5 larger than the limiting linewidth reported by Mali *et al.*[19] for stoichiometric $YBa_2Cu_3O_{6+x}$ ($x = 1$). The smallest width reported by these authors is 90 kHz in superconducting powders. They find that 40 kHz are due to crystal defects other than oxygen stoichiometry. Since this residual width is larger in antiferromagnets our value indicates a good quality of the Gd substituted samples. Previous to the nuclear relaxation times we remeasured the Cu spectra and found good agreement with the earlier results.

The samples were placed in the coil of a LC resonance circuit and immersed in liquid He. The temperature was regulated by means of the He pressure and measured with a calibrated carbon-glass resistance thermometer adjacent to the sample in the bath. During the sampling period of an echo the temperature stability was better than 5 mK.

The spin echoes were detected with a homemade coherent broadband spectrometer. The intensities were evaluated by Fourier-transformation of signals sampled up to 5000 times. The enhancement factors η were determined from the dependence of the echo intensity at resonance frequency I on the effective rf field at the nucleus ηH_1 for a $\tau - 2\tau$ pulse sequence:

$$I = C\eta \sin^3(\gamma\eta\mu_0 H_1 \tau). \tag{2.1}$$

C contains the spectrometer sensitivity, the number of nuclei, temperature, and frequency. The enhancement occurs not only for the rf field at the nucleus but also for the signal induced in the pickup coil, since we find that the signal intensity increases with η in moderate external fields. In the absence of an absolute calibration of H_1 we set $\eta = 1$ at zero external field and 4.2 K. If not stated otherwise the data for η discussed below were taken for the Cu(2) site at a constant frequency of 99 MHz in the nonsuperconducting sample x=0. In this way the broad NMR spectrum in external fields of this site allows measurements of the Cu echo in various fields without tuning to different frequencies. No attempt was made to correct for a change in the transition probabilities due to different transitions and isotopes contributing to the signal. Since the external field is always small compared to the Cu hyperfine field such effects are small. The enhancement factors in the powder are only homogeneous in zero or large external field. At intermediate fields Eq. (2.1) yields comparably poor fits to the dependence of the intensity on the rf field because of the restriction to a single value for η. The enhancement factor is probably distributed in the powder samples due to the random orientation of the field with respect to the grains. Since the H_1 sweeps contain not at all external fields enough structure for a three-parameter fit required to analyze a distribution in η, we give only the η appropriate to fit the data near the first intensity maximum with Eq. (2.1). This will give a conservative estimate of η. When it deviates from 1 larger values are clearly present.

T_1 was determined from the decay of the stimulated echo. The results agreed with a least squares fit to saturation recovery measurements but this method was preferred since only two prameters have to be determined in the fit. The decay is similar to the one of the Hahn echo used to measure T_2, single exponential for the pure NQR of the Cu(1) and the Cu(2) sites in superconducting samples in zero field with a time constant $T_1/3$. The relaxation for the $\pm 1/2$ transition of the Cu(2) sites in nonsuperconducting samples is well described with a single T_1 within the Redfield theory by $\exp(-t/T_1) + 9\exp(-6t/T_1)$. T_1 is in both cases the time constant for the spin-1/2 system.

In order to verify that the relaxation is dominated by magnetic rather than electric quadrupole interactions we checked that the ratios $^{69}T_{1,2}/^{71}T_{1,2}$ of the two Ga isotopes, which occupy the Cu(1) sites in $GdSr_2GaCu_2O_7$, agree to $(^{71}\gamma/^{69}\gamma)^2 = 1.615$ in our temperature range. The difference of the gyromagnetic constants and nuclear quadrupole moments is larger for the Ga than for the Cu isotopes, allowing a clearer distinction of the two relaxation mechanisms. In $YBa_2Cu_3O_{6+x}$ we find relaxation times an order of magnitude longer than the ones observed in $GdBa_2Cu_3O_{6+x}$, which is further evidence that the relaxation of the CuO planes is dominated by the fluctuations of the Gd moments. The difference is

smaller for the Cu(1) sites, due to their larger distance and higher symmetry with respect to the Gd layers.

III. RESULTS AND DISCUSSION

A. Spin configuration

Below the Néel temperature of the Gd layer a marked decrease of the relaxation rates was observed on all Cu sites. We were able to observe the resonance at all temperatures and could not identify any critical contributions to the fluctuations, independent of the Cu position and its oxygen coordination at the Cu(1) sites. This is in accord with the absence of any line splitting or broadening within the Cu spectrum from static hyperfine fields in the ordered state at low temperatures. A cancellation of the dipolar fields from Gd moments parallel to the c axis occurs at the Cu sites only if the antiferromagnetic unit cell is doubled in both directions of a Gd plane [$q_c' = (\frac{1}{2}, \frac{1}{2})$ in the plane] (see Fig. 1). This is the structure detected in neutron diffraction.[5,10] With ferromagnetic chains of nearest neighbors in the plane [$q_c' = (\frac{1}{2}, 0)$] the cancellation requires that the spins are aligned along the ferromagnetic direction in the plane. Since this is the case for the configuration favored by the dipolar interaction we cannot exclude this arrangement from our data without direct observation of the Gd resonance. Such a cancellation of the dipolar fields does not occur at the asymmetric Ga sites in $GdSr_2GaCu_2O_7$. There a static line broadening below T_N and a critical contribution to the nuclear Ga relaxation was observed.[20]

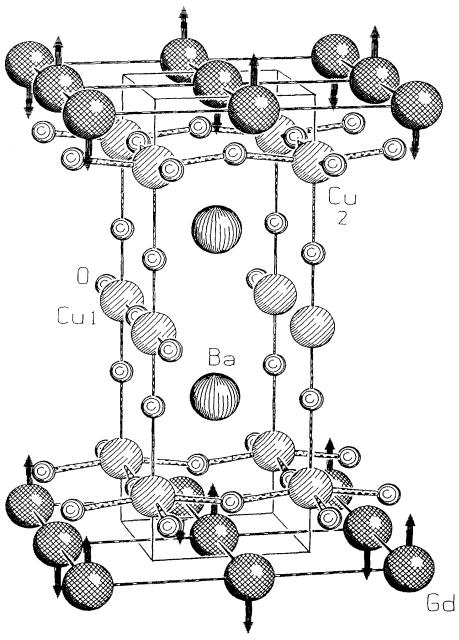

FIG. 1. Magnetic structure of the Gd sublattice in $GdBa_2Cu_3O_{6+x}$. The three different oxygen coordinations shown for the Cu(1) site can be distinguished by their NQR frequency. For the superconducting samples the structure is orthorhombic with $a = 3.823$, $b = 3.887$, $c = 11.680$ Å.

B. Noncritical fluctuations: T_1

Within the theory of Kubo and Tomita[21] the spin-lattice relaxation rate can be calculated from the Fourier transform of the static spin-spin correlation function $\mathbf{S}(\mathbf{q}, t = 0)$ of the fluctuations, the hyperfine coupling tensor $\mathcal{C}(\mathbf{q})$ for a fluctuation with wave vector $\mathbf{q}$, and the characteristic frequency $\Omega(\mathbf{q})$ according to

$$T_1^{-1} = \sum_{\mathbf{q}\in \mathrm{BZ}} \sum_{i,j=x,y,z} C_{ij}(\mathbf{q}) S_i(\mathbf{q})/\Omega_i(\mathbf{q}). \tag{3.1}$$

The coupling tensor $\mathcal{C}(\mathbf{q})$ selects only the components of the vector $\mathbf{S}(\mathbf{q})$ responsible for fields perpendicular to the axis of quantization. In the following we omit the index for these fluctuations and characteristic frequencies. There are a number of simplifying assumptions involved in Eq. (3.1). The most common approach to establish a relation between T_1^{-1} and the correlation functions of a microscopic theory is time dependent perturbation theory with the fluctuating fields at the nucleus as a small parameter. As discussed in the textbooks this is justified in the weak-collision limit, i.e., for large resonance frequencies ($\omega_0 T_{1,2} \gg 1$), which applies in our experiments, or for a large characteristic frequency of the motion under consideration ($\Omega_c T_{1,2} \gg 1$), which will not hold in the case of critical slowing down. In the derivation of Eq. (3.1) the Fourier component of the dynamic correlation function at the NMR frequency, $S(\mathbf{q}, \omega_0)$, is replaced by the static structure factor $S(\mathbf{q}) = 1/2\pi \int S(\mathbf{q}, \omega) d\omega$ times the spectral density at $\omega_0 \approx 0$:

$$S(\mathbf{q}, \omega) = S(\mathbf{q}) J_q(\omega) \approx S(\mathbf{q}) J_q(0). \tag{3.2}$$

This is valid for fast motions of the moments compared to the resonance frequency and will also break down for the critical mode $q = q_c$ near T_c. Finally the spectral density at zero frequency is given by the mean of the time dependent part $g_{\mathbf{q}}(t)$ of the spin-spin correlation function $\mathbf{S}(\mathbf{q}, t) = \mathbf{S}(\mathbf{q}) g_{\mathbf{q}}(t)$:

$$J(\omega = 0) = \frac{1}{2\pi} \int e^{-i\omega t} g_{\mathbf{q}}(t) dt = \frac{1}{2\pi} \int g_{\mathbf{q}}(t) dt \tag{3.3}$$

which in turn is characterized by the correlation time, $\Omega(\mathbf{q})^{-1}$. An explicit form of $g_{\mathbf{q}}(t)$ is difficult to calculate and will depend on the model involved (spin-wave approximation, high temperature expansion), but for the noncritical modes the characteristic frequency $\Omega(\mathbf{q})$ is expected to be a slowly varying function of temperature without critical behavior near T_c.[22] In the following we assume that $\Omega(\mathbf{q} \neq \mathbf{q}_c)$ is independent of temperature.

The hyperfine coupling tensor $\mathcal{C}(\mathbf{q})$ may in principle be calculated exactly from the lattice geometry and the spin arrangement corresponding to the fluctuation of wave vector $\mathbf{q}$. The resulting field at the nucleus under consideration,

$$H_{loc} = -\frac{\gamma_e \hbar}{4\pi} \sum_i \left(\frac{\mathbf{S}_i}{r_i^3} - 3 \frac{(\mathbf{r}_i \mathbf{S}_i) \mathbf{r}_i}{r_i^5} \right) - \sum_i \frac{\mathcal{A}}{\mu_0 \gamma} \mathbf{S}_i, \tag{3.4}$$

consists of a dipolar contribution of the spins $\mathbf{S}_i$ at lattice sites $\mathbf{r}_i$ with an electronic gyromagnetic ratio γ_e, and of a hyperfine field described by the coupling tensor $\mathcal{A}$, which is usually assumed to be isotropic and only nonzero for nearest neighbors.

The main contribution is expected from the dipolar interaction. In order to confirm this we compare T_1 well above T_N with the linewidth of the Gd resonance at room temperature in ESR.[14] We make the further assumptions of a simple exponential decay of the correlations with the decay rate $\Omega(\mathbf{q})$,[23] and take only the dipolar field for uncorrelated, isotropic fluctuations of the Gd moments into account to estimate the field fluctuations at the Cu(1) site. In this way we find $T_1^{-1} \approx 70$ Hz from $\Omega_{\mathrm{ESR}}^{-1} = 4 \times 10^{-11}$ s, in reasonable agreement with our experimental value of 300 Hz at 4.2 K. We therefore neglect the hyperfine contribution to $\mathcal{C}(\mathbf{q})$ in the discussion below. Because of the tensor character of the dipolar interaction $\mathcal{C}(\mathbf{q})$ is usually calculated numerically. The coupling will clearly vanish for all wave vectors $\mathbf{q}$ with zero static dipolar fields at the Cu sites. In this case the contributions from $\mathbf{q} = \mathbf{q}_c$ vanish and the underlying assumptions for Eq. (3.1) should be valid in the whole temperature range.

Since the characteristic frequencies in Eq. (3.1) are not known we did not attempt the numerical evaluation and discuss only the temperature dependence of T_1^{-1}. This is shown in Fig. 2 for the Cu(1) sites and three oxygen concentrations. The relaxation rate drops by approximately a factor of 6 at T_N for all oxygen concentrations, without any maximum indicating a coupling to the critical fluctuations. With C_{ij} and Ω temperature independent it may be seen from Eq. (3.1) that T_1^{-1} directly reflects the temperature dependence of the structure factor $S(\mathbf{q})$, integrated with some $\mathbf{q}$-dependent weight function. The drop in T_1^{-1} at T_N is, thereby, due to a shift of the weight in the Brillouin zone in favor of wave vectors near q_c. On the right-hand side of Fig. 2 it is seen that a quite satisfying fit over the whole range of variation of T_1^{-1} is achieved with a linear dependence of $S(\mathbf{q})$ on $t \ln t$, where t is the reduced temperature. Table I gives the transition temperatures and fit parameters corresponding to the lines in the figure.

This temperature dependence was first proposed as

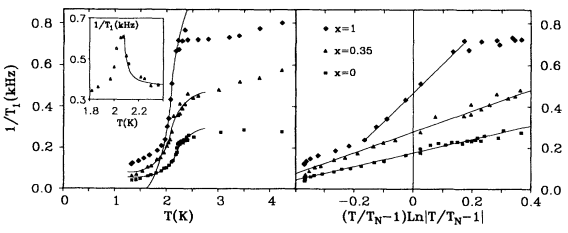

FIG. 2. ^{63}Cu(1) spin-lattice relaxation rate at 22.4 and 23.7 MHz (four- and threefold coordination) for $x \neq 0$ and 30.1 MHz (twofold coordination) for $x = 0$ in zero field temperature. The lines are fits to Eq. (3.1), valid for 2D and 3D Ising systems. The inset shows the critical contribution to the T_1^{-1} of Ga in $GdSr_2GaCu_2O_7$ together with a line for the 2D Ising critical behavior.

TABLE I. Transition temperatures and parameters of the temperature dependence [Eq. (3.5)]. Note that the experimental a and b due to Eq. (3.1) are weighted sums of the Fourier transforms of $a(\mathbf{r}), b(\mathbf{r})$.

Sample (x)	T_N (K)	$\tilde{a}$ (kHz)	$\tilde{b}$ (kHz)	$-\tilde{a}/\tilde{b}$
0	2.19	0.17	−0.33	0.51
0.35	2.09	0.28	−0.53	0.53
1.0	2.09	0.47	−1.4	0.34
Ga	2.06	—	—	—

an approximant for the correlation function $G(r)$ in real space by Fisher, Sykes, and Burford[24,25] for 2D and 3D Ising antiferromagnets:

$$G(\mathbf{r}) = a(\mathbf{r}) + b(\mathbf{r})(1 - T/T_N)\ln(1 - T/T_N). \quad (3.5)$$

In the relaxation rate the Fourier transform is relevant, which shows (for $\mathbf{q} \neq \mathbf{q}_c$) the same temperature dependence. While the absolute values of $a(\mathbf{q}), b(\mathbf{q})$ are unknown, Fisher *et al.* give an estimate of the ratio $a(q = 0)/b(q = 0) \approx 0.56$ and ≈ 3.1 for 2D and 3D systems, respectively. The experimental data are within the errors in accord with the 2D value, but we emphasize that the analytic form of the spatial dependence of a and b in Eq. (3.5) is unknown and it is by no means clear that the ratio of the weighted sums $\tilde{a}, \tilde{b}$ of $a(q)$ and $b(q)$ is the same as that for $q = 0$. We note in addition that the slope $\tilde{b}$ above and below T_N is the same, which is also in general agreement with the theoretical predictions of Fisher and Sykes[24] for the 2D system but not the case in three-dimensional Ising systems.

Qualitatively the same temperature dependence of the relaxation rates was observed at the Cu(2) sites for $x = 0$, but with T_1^{-1}=T_2^{-1}=60 kHz above T_N and only a small, rather broad maximum at T_N ($\Delta T \approx 0.2$ K). The Cu(2) site is, in contrast to the Cu(1) site, sensitive to transverse fluctuations of the Gd moments at $\mathbf{q}_c$. This result indicates, thereby, that the Ising anisotropy also holds for the critical fluctuations.

The fact that the $^8S_{7/2}$ Gd moments with the large, pure spin moment show Ising behavior can be understood by an anisotropy crossover for the 2D (or 3D) Heisenberg system. We propose that the leading term in the Hamiltonian of the Gd sublattice corresponds to a 2D Heisenberg antiferromagnet with three spin components. Assuming a Curie-Weiss susceptibility χ in the high temperature limit, a temperature independent T_1^{-1} is expected from Eq. (3.1), if $S(\mathbf{q}, t = 0) \propto \chi T$ is inserted from the fluctuation dissipation theorem. This is in general agreement with the experiment. The isotropic 2D system has no phase transition but any Ising-type anisotropy or 3D coupling between the planes will induce one. Pich and Schwabl showed recently that even a dipolar anisotropy alone is sufficient to induce the transition.[26] The transition temperature depends only near the bicritical point in the H-T phase diagram on the size of the anisotropy. Outside this region the variation is small, following[27] $T_N \propto (H_a/H_{\mathrm{ex}})^{0.04}$ or[26] $\ln(H_a/H_{\mathrm{ex}})$. This is in accord with the observation of a constant T_N for different prop-

erties of the intermediate CuO layers (Table I). Strong variations with x were reported in contrast to this for other RE elements like Nd or Sm.[28,29]

The dipolar anisotropy field may be inferred from the Gd spin configuration. As indicated above the dipolar forces favor a spin configuration with the moments in the a-b plane aligned ferromagnetically along one nearest-neighbor direction.[4] The observed antiferromagnetism along the a and b axes is, therefore, due to an exchange coupling. We assume an isotropic coupling with respect to the orientation of the antiferromagnetic magnetization vector. The dipolar interaction gives rise to an anisotropy. Given the antiparallel orientation of all nearest neighbors in a plane it favors the observed spin alignment along the c axis. We find the anisotropy field $\mu_0 H_a = 0.2$ T from the difference in dipolar energy for the orientation of the antiferromagnetic magnetization in the a-b plane and collinear to c, respectively.

According to the universality hypothesis corrections to the overall Hamiltonian are important near $T = 0$ and $T = T_c$. The width of the temperature interval where a crossover to a lower spin or higher lattice dimensionality can be observed depends on the strength of the corresponding perturbation. In the present case the dipolar anisotropy and a 3D coupling may influence the fluctuations of the Gd moments. Since the fluctuations are of the Ising-type we conclude that the anisotropy is the larger correction to the 2D Heisenberg AF. We found no evidence for a crossover to 3D fluctuations near T_N, maybe due to an insufficient temperature resolution. Such a 2D Ising behavior is in accord with the large fluctuations of the moments well above and below T_N, but in contrast to the absence of 2D fluctuations or 2D ridges in the neutron scattering reported by Mook *et al.*[9,15,5] The comparably narrow temperature interval where Eq. (3.5) holds for the oxygen-rich sample (Fig. 2) indicates a reduced anisotropy for the Gd moments in the superconductors.

A similar Ising-type anisotropy induced by the dipolar interaction is observed in the classical 2D Heisenberg antiferromagnet K_2MnF_4. Although the anisotropy parameter H_a/H_{ex} in this system is nearly a factor of 40 smaller the ratio $\alpha = k_B T_N/[JS(S+1)] \approx 1.2$ is of the same order of magnitude as for $GdBa_2Cu_3O_{6+x}$ ($\alpha \approx 2.0$). This scaling shows that T_N depends only weakly on the anisotropy, in accord with the prediction mentioned above.

We are not able to identify the origin of the increasing T_1^{-1} with the oxygen concentration shown in Fig. 2. The characteristic frequency as well as the static structure factor in Eq. (3.1) may depend on the susceptibility of the adjacent CuO layers. The hyperfine coupling tensor will also depend on x, since it was defined to project from the fluctuations the contributions responsible for fields perpendicular to the quantization axis. For the Cu(1) sites with two oxygen neighbors in the nonsuperconducting samples it is clear from symmetry that the c axis is the major axis of the electric field gradient (EFG). This component of the EFG reduces for the fourfold coordination to nearly zero,[30] resulting in an asymmetry parameter $\eta = 1$ and a relaxation connecting different eigenstates. This change of symmetry is apparently not the leading contribution to the x dependence of T_1^{-1}, since T_2^{-1} also increases with x, but is sensitive to the fluctuating fields along the quantization axis.

As noted above a static line broadening was observed in $GdSr_2GaCu_2O_7$ at the Ga site, corresponding to a dipolar field of $\approx$ 100 mT. The hyperfine coupling to the critical mode $\mathcal{C}(\mathbf{q} = \mathbf{q}_c)$ is nonzero, due to the shift of the Ga site out of the symmetric position in center of the unit cell (Fig. 1). Together with the static fields we observe a critical contribution to the relaxation times $T_{1,2}$, see the inset to Fig. 2 for T_1^{-1}. The peak is too small to allow a detailed evaluation of the dynamical critical exponent, but consistent with the discussion above the exponent -1.5 for the 2D Ising system[31] gives the best approximation of the data (line in the inset). A similar behavior might be expected for the Cu(1) site at the end of an O-filled chain, but T_1^{-1} of the line at 24 MHz is within the error the same as for all Cu(1) sites.

C. Critical field: T_2

In Fig. 3 the spin-spin relaxation rates for the Cu(1) sites in antiferromagnetic $GdBa_2Cu_3O_{6+x}$ are shown. Superimposed on the decrease at T_N, which is similar to the shape of T_1^{-1}, there is a peak at the phase transition, which is especially in zero field remarkably narrow ($\approx$ 60 mK) and high compared to the noncritical background. The peak only occurs in T_2^{-1} and only at the Cu(1) sites in nonsuperconducting samples (see inset for the superconducting sample x=1), but there independent of the oxygen coordination (the NQR frequency). It was not observed on the Cu(2) sites, where it might be hidden in the comparably high noncritical relaxation rates ($\approx$ 60 kHz at T_N). With increasing field applied to the nonoriented powder the peak broadens and decreases, but as seen in the figure it can be used at least up to 2 T to determine the critical temperature and the critical field H_c.

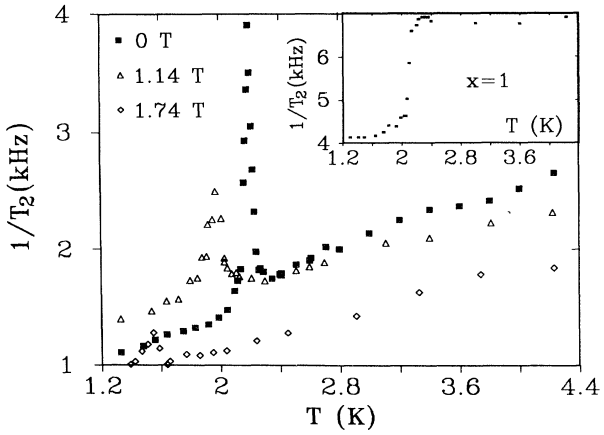

FIG. 3. Temperature dependence of T_2 for ^{63}Cu(1) sites in different fields in the semiconducting sample ($x = 0$). The peak occurs at the phase transition of the Gd sublattice. It is not observed in superconducting samples (see inset).

The spin-echo decay is determined by three processes, namely a contribution from T_1^{-1}, the homogeneous linewidth due to dipolar and Suhl-Nakamura interactions, and the contributions from fluctuations, which are related to T_2^{-1} by an expression similar to Eq. (3.1). The dipolar contribution to the homogeneous Cu(1) linewidth is independent of temperature and in the order of 1 kHz. The fluctuations $\mathbf{S}(\mathbf{q},\omega)$ contributing to T_2^{-1} have extremely low frequencies and lead with the coupling tensor $\mathcal{C}(\mathbf{q})$ to fields along the quantization axis. The noncritical temperature dependent background in T_2^{-1} in Fig. 3 is a sum of the T_1^{-1} contribution and these fluctuations. It can be described by const $\cdot T_1^{-1}$(T), where the constant varies with the oxygen concentration between 4.5 (x=1) and 7 (x=0). It is difficult to draw conclusions on the anisotropy of the fluctuations from this result, because the q dependence of the hyperfine-coupling enters in the integration of Eq. (3.1). If only noncritical contributions are involved the constant should be temperature independent and of the observed order of magnitude.

The absence of any maximum in T_1^{-1} shows that the mechanism responsible for the peak in T_2^{-1} is very anisotropic. We would like to comment briefly on various proposals in the literature to describe similar phenomena in other systems. Bucci and Guidi found a very anisotropic linewidth for the planar ^{19}F site at the phase transition of the planar antiferromagnet K_2MnF_4. They ascribe this to contributions from fluctuations near the critical wave vector q_c, which are not totally suppressed by the vanishing $\mathcal{C}(\mathbf{q})$. The observed anisotropy arises from the anisotropic coupling to the F site in the middle of two magnetic Mn ions.[32] In contrast to this and to our experimental result the dipolar coupling of the Gd moments to Cu sites contributes for fluctuations with $\mathbf{q}$ near $\mathbf{q_c}$ mainly to T_1^{-1}, i.e., the fluctuating fields are perpendicular to the quantization axis. Furthermore the hyperfine coupling near q_c rises proportional to $(q-q_c)^2$, which should be sufficiently slow to suppress critical contributions from all known dynamical critical exponents, including the 2D Ising fluctuations. Moriya proposed for MnF_2 a mechanism for a large homogeneous linewidth at T_N due to the indirect coupling of nuclear spins via the electronic susceptibility.[23] In the low temperature regime this corresponds to the well-known Suhl-Nakamura interaction by exchange of virtual spin waves. This mechanism is rather attractive because it conserves energy and influences, thereby, only T_2^{-1}, but it involves the same symmetry forbidden coupling between the antiferromagnetic fluctuations and the Cu spin as the contribution from critical modes at $q = q_c$ in Eq. (3.1) and is therefore also expected to be small. Birgenau *et al.* observed in the inelastic neutron scattering of K_2NiF_4 a longitudinal, diffusive critical mode, which was discussed by Heller for MnF_2.[33,34] Halperin and Hohenberg predicted within a hydrodynamical theory for the planar antiferromagnet low frequency spin waves at long wavelengths for all temperatures up to the paramagnetic phase[35] and Huber pointed more recently to a central peak in the longitudinal spin-autocorrelation function of quasi-2D planar magnets like the present system.[36] In all these cases the anisotropy in the relaxation is due to the fluctuations. We are not aware of an analysis of the temperature dependence of the dynamic correlation functions detailed enough to allow comparison with our data. In addition the applicability of these models is rather unclear, since the planar symmetry would only be induced by an external field in the present Ising system. Finally we would like to note that the peak in T_2^{-1} might be connected with the low frequency fluctuations observed in nonsuperconducting $GdBa_2Cu_3O_{6+x}$ by μSR.[15]

D. Spin-flop transition: η

In antiferromagnets with an easy axis anisotropy there occurs in the antiferromagnetic phase in external fields along the easy axis the spin-flop transition. At the spin-flop field H_{sf} the energy of the configuration with both sublattice magnetizations parallel to the field becomes unfavorable compared to a configuration of canted spins nearly perpendicular to the field. The spin-flop transition is frequently broadened especially in 2D antiferromagnets by domain effects or misorientation of the field, which clearly occurs in the current powder samples.[37]

At the spin-flop transition a small change in the field causes a large rotation of the sublattice magnetizations. In ferromagnets and canted antiferromagnets this leads to the well-known effect of enhanced internal rf fields, measured by the enhancement factor

$$\eta_{\perp,\parallel} = \frac{dH_{\mathrm{HF}}}{dH_1} = \alpha M \frac{d(\sin\theta)}{dH_1}. \tag{3.6}$$

$H_{\mathrm{HF}} = \alpha M$ is the hyperfine field at the nucleus due to the sublattice magnetization M and hyperfine coupling constant α. When M is rotated by θ due to the rf field H_1 the hyperfine field follows this rotation, creating a rf component perpendicular to the original H_{HF}. $\eta_{\parallel}$ and $\eta_{\perp}$ denote a parallel and perpendicular arrangement of rf field and static external field, respectively.

We observed no enhancement ($\eta = 1$) at high fields and only a very small but systematic decrease of η with temperature in zero field. As can be seen in Fig. 4, large enhancement factors $\eta_{\parallel}$ and $\eta_{\perp}$ up to 15 are present at the Cu(2) site in nonsuperconducting $GdBa_2Cu_3O_{6+x}$ at low temperatures and in fields up to 2 T. Significant enhancement factors were observed only for the Cu(2) resonance in the nonsuperconducting samples and with Gd on the RE layer. No enhancement was observed for any Cu site when $x > 0.4$ (superconductors), for the Cu(1) sites, or in antiferromagnetic $YBa_2Cu_3O_{6+x}$.

A well-resolved maximum of $\eta_{\parallel}$ and $\eta_{\perp}$ (not shown) was observed at an external field $\mu_0 H_0 = 0.6$ T, even at 4.23 K. Below T_N we associate this maximum with the large rotation angles occurring at the spin-flop transition in the Gd sublattice due to H_1. In fields above ≈ 1 T $\eta_{\perp}$ decreases like $1 + H^*/H_0$ with a field constant $\mu_0 H^* \approx 7$ T. Below T_N the enhancement factor at 0.6 T is for both orientations high and constant within the experimental resolution up to T_N. While $\eta_{\perp}$ displays a broad maximum above T_N, $\eta_{\parallel}$ drops discontinuously at T_N to a value near 1 and reaches a maximum again

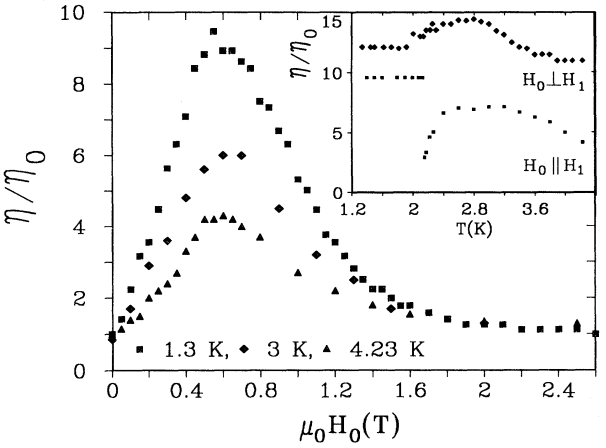

FIG. 4. Enhancement of the rf field at the antiferromagnetic Cu(2) sites vs external field for parallel arrangement $H_0 \| H_1$ of rf and static field. The inset shows the temperature dependence at 0.6 T, where the maximum enhancement is found for parallel as well as perpendicular excitation.

at 2.8 K. Both $\eta_\perp$ and $\eta_\parallel$ are still large well above T_N, but the parallel enhancement approaches the high temperature limiting value of one more rapidly than $\eta_\perp$.

While this temperature dependence strongly resembles that of the homogeneous susceptibilities of an antiferromagnet, the origin of the enhancement is not fully understood at the moment. From Eq. (3.6) it is seen that η is proportional to the susceptibility of the rotation of the sublattice magnetization in the CuO planes. These are antiferromagnetic and, due to their large exchange coupling, not in a canted state, so no enhancement can occur within this lattice for homogeneous fields. This is in accord with the fact that no enhancement was observed with Y at the RE site. The enhancement is also not due to the direct homogeneous dipolar field from the Gd moments at the Cu(2) site, since no enhancement is observed in the superconducting samples. This may also be seen from the homogeneous magnetization in the Gd sublattice, which produces in the spin-flop state a field ≤ 0.3 T at the Cu(2) site. We compare this with the total change in the hyperfine field projected to the field direction when the static field is applied. According to Eq. (3.6) we can estimate this by integration of $\eta_\parallel$ with respect to the field. At 1.3 K this amounts to ≈ 7 T, which is large compared to the Gd field but within the experimental error equal to the field constant in $\eta_\perp$ indicated above.

The most probable mechanism for the enhancement arises in our opinion in the spin-flop state of the Gd moments. In this phase the Gd moments display an easy-plane anisotropy with a field-dependent component of the moments in the a-b plane. As discussed in the Introduction such a configuration leads to a staggered field at the Cu(2) sites, which we estimate to ≤ 0.7 T. The external rf field couples to the homogeneous component of the Gd magnetization and generates in this way an oscillating *staggered* field at the Cu(2) sites. The large enhancement factors are in this model due to a rotation of the Cu moments in the a-b plane, where their anisotropy is small. The large change in the hyperfine field and the field constant H^* discussed above correspond in this model to the hyperfine field at the Cu nucleus of 7.8 T in the antiferromagnetic state. This explains why the Gd moments as well as the antiferromagnetism in the CuO planes are necessary for the effect. It is, on the other hand, within this model difficult to understand the large enhancement factors in the paramagnetic state of the Gd above T_N and H_c, where no static antiferromagnetic component of the Gd magnetization is available to produce the staggered field. The very low frequency fluctuations reported in the μSR work might be connected with this enhancement factor as well.

E. Phase diagram

In Fig. 5 we show the H-T phase diagram of the Gd sublattice as determined from this work. Two additional values of H_c from specific heat and magnetization measurements have been included.[7,13] For the ground state of an anisotropic Heisenberg antiferromagnet one finds

$$H_{sf}^2 = H_c H_a, \tag{3.7}$$

$$H_c = 2H_{ex} \pm H_a. \tag{3.8}$$

$\mu_0 H_{ex} = 2zJS/g\mu_B$ is the exchange field. The sign in the equation for the critical field depends on the orientation of the external field (+ for $H_0 \perp c$ axis). We extrapolate the critical field $\mu_0 H_c(T=0) \approx 3.1$ T by means of the empirical Bienenstock formula $H_c(T)/H_c(T=0) = [1 - T_N(H)/T_{N0}]^\phi$ for the critical field. The solid line in Fig. 5 represents this dependence for $\phi = 0.86$, valid for a 2D square lattice.[38] The temperature dependence of the spin-flop field (0.6 T) is small, so we find for the anisotropy field $\mu_0 H_a = 0.12$ T and for the exchange field $\mu_0 H_{ex} = 1.5$ T. This is in fair agreement with the result of Nakamura *et al.* from ESR.[14] The anisotropy field is also in good agreement with the dipolar anisotropy calculated above for the spins along the c axis.

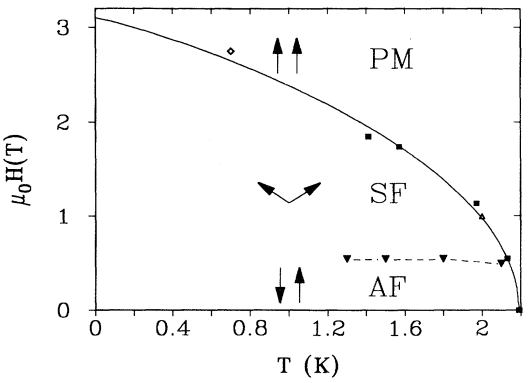

FIG. 5. Magnetic phase diagram of $GdBa_2Cu_3O_{6+x}$ with x=0. The critical field from NMR is determined from T_2, the spin-flop transition from the enhancement factor. The full line is according to the empirical Bienenstock formula (see text). △, specific heat (Ref. 7) ◇, magnetization (Ref. 13).

IV. CONCLUSION

We studied the nuclear relaxation rates T_1^{-1}, T_2^{-1} and the enhancement factor η of the Cu(1) and Cu(2) sites in $GdBa_2Cu_3O_{6+x}$ near the antiferromagnetic phase transition of the Gd sublattice. The critical and the spin-flop field in the magnetic phase diagram were determined from T_2 and η, respectively. With these values we find $\mu_0 H_{ex} = 1.5$ T for the in-plane exchange and $\mu_0 H_a = 0.1$ T for the anisotropy field at $T = 0$. The temperature dependence of T_1 and of a contribution to T_2 is in good agreement with theoretical predictions for Ising-systems. The temperature interval at T_N where we observed the Ising-type fluctuations is broader than 1 K and in general accord with the dipolar anisotropy for the nonsuperconducting samples ($x < 0.4$), and significantly smaller for the superconductors ($x > 0.4$). We presented evidence for a 2D magnetism of the Gd moments: the ratio $\tilde{a}/\tilde{b}$ of the Ising parameters in Table I, the equal slope $\tilde{b}$ above and below T_N, the critical contributions to the Ga relaxation in $GdSr_2GaCu_2O_7$, and the maxima in $\eta_\perp$ and $\eta_\parallel$ well above T_N are all best described within the 2D Ising model.

As noted above the 2D Ising model is in accord with specific heat and Mössbauer data but in contrast to results from neutron diffraction. The origin of the marked peak in the spin-spin relaxation observed only at the Cu(1) site in nonsuperconducting samples is another open question. Furthermore the mechanism of the enhancement factor especially in the paramagnetic region remains an interesting problem, which should be adressed within future work on single crystals.

ACKNOWLEDGMENTS

We are indebted to M. Buchgeister (Dresden) and G. Roth (Karlsruhe) for providing the samples. We gratefully acknowledge the fruitful discussions and the possibility to conduct this work in the group of J. Kötzler in Hamburg. K.N. was supported by a grant of the University of Hamburg, the work was supported by the Deutsche Forschungsgemeinschaft.

[1] V. Nekvasil, J. Magn. Magn. Mater. (to be published).
[2] B. W. Lee, J. M. Ferreira, Y. Dalichaouch, M. S. Torikachvili, K. N. Yang, and M. B. Maple, Phys. Rev. B **37**, 2368 (1988).
[3] W-H. Li, J. W. Lynn, S. Skanthakumar, T. W. Clinton, A. Kebede, C.-S. Jee, J. E. Crow, and T. Mihalisin, Phys. Rev. B **40**, 5300 (1989).
[4] H. Sen, Phys. Lett. A **129**, 131 (1988).
[5] H. A. Mook, D. McK. Paul, B. C. Sales, L. A. Boatner, and L. Cussen, Phys. Rev. B **38**, 12 008 (1988).
[6] B. D. Dunlap, M. Slaski, Z. Sungaila, D. G. Hinks, K. Zhang, C. Segre, S. K. Malik, and E. E. Alp, Phys. Rev. B **37**, 592 (1988).
[7] K. Kadowaki, H. P. van der Meulen, J. C. P. Klaasse, M. van Sprang, J. Q. A. Koster, L. W. Roeland, F. R. de Broer, Y. K. Huang, A. A. Menovsky, and J. J. M. Franse, Physica B **145**, 260 (1987).
[8] C. Meyer, H.-J. Bornemann, H. Schmidt, R. Ahrens, D. Ewert, B. Renker, and G. Czjzek, J. Phys. F **17**, L345 (1987).
[9] H.-J. Bornemann, G. Czjzek, D. Ewert, C. Meyer, and B. Renker, J. Phys. F **17**, L337 (1987).
[10] M. Guillaume, P. Fischer, B. Roessli, P. Allenspach, and V. Trounov, Physica C **235–240**, 1637 (1994).
[11] D. Thiery, L. Walz, H. G. von Schnering, T. Chattopadhyay, P. J. Brown, W. Wirges, K. Fischer, and H. Maletta, Z. Phys. B **80**, 177 (1990).
[12] H. Lütgemeier, *Proceedings of the 26th Zakopane Summer School on Physics* (World Scientific, Singapore, 1991), p. 264. Kumagai *et al.* report, on the other hand, no influence of Al on the antiferromagnetic Cu structure [K. Kumagai, T. Takatsuka, and A. Yamanaka, J. Magn. Magn. Mater. **104-107**, 577 (1992)].
[13] I. Oguro, T. Tamegai, and Y. Iye, Physica B **148**, 456 (1987).
[14] F. Nakamura, Y. Ochiai, H. Shimizu, and Y. Narahara, Phys. Rev. B **42**, 2558 (1990).
[15] C. Niedermayer, H. Glückler, A. Golnik, U. Binninger, M. Rauer, E. Recknagel, J. I. Budnick, and A. Weidinger, Phys. Rev. B **47**, 3427 (1993).
[16] I. Heinmaa, H. Lütgemeier, S. Pekker, G. Krabbes, and M. Buchgeister, Appl. Magn. Res. **3**, 689 (1992).
[17] K. Nehrke and M. W. Pieper, Physica C **235–240**, 1657 (1994).
[18] M. Buchgeister, Ph. D. thesis, University of Bonn, FRG, 1991.
[19] H. Schiefer, M. Mali, J. Roos, H. Zimmermann, D. Brinkmann, S. Rusiecki, and E. Kaldis, Physica C **162-164**, 171 (1989).
[20] M. W. Pieper, Physica C **190**, 261 (1992).
[21] R. Kubo, K. Tomita, J. Phys. Soc. Jpn. **9**, 888 (1954).
[22] F. Borsa and A. Rigamonti, in *Magnetic Resonance of Phase Transitions*, edited by F. J. Owens, C. P. Poole, and H. A. Farach (Academic, New York, 1979).
[23] T. Moriya, Prog. Theor. Phys. **28**, 371 (1962).
[24] M. F. Sykes and M. E. Fisher, Physica **28**, 919 (1962); **28**, 939 (1962).
[25] M. E. Fisher and R. J. Burford, Phys. Rev. **156**, 583 (1967).
[26] C. Pich and F. Schwabl, Phys. Rev. B **49**, 413 (1994).
[27] K. Binder and D. P. Landau, Phys. Rev. B **13**, 1140 (1976).
[28] K. N. Yang, J. M. Ferreira, B. W. Lee, M. B. Maple, W.-H. Li, J. W. Lynn, and R. W. Erwin, Phys. Rev. B **40**, 10 963 (1989)
[29] P. Allenspach, B. W. Lee, D. Gajewski, M. B. Maple, S. I. Yoo, and M. J. Kramer, J. Appl. Phys. **73**, 6317 (1993).
[30] D. J. Singh, K. Schwarz, and P. Blaha, Phys. Rev. B **46**, 5849 (1992); the principal axes of the EFG for the threefold coordination are also along the tetragonal axes [S. Schmenn *et al.* (unpublished)].
[31] H. Benner and J. P. Boucher, in *Physics and Chemistry of*

Materials with Low-Dimensional Structures, edited by L. J. deJongh (Kluwer Academic, Dordrecht, 1990), Vol. 9.
[32] C. Bucci and G. Guidi, Phys. Rev. B **9**, 3053 (1974).
[33] R. J. Birgeneau, J. Skalyo, and G. Shirane, Phys. Rev. B **3**, 1736 (1971).
[34] M. P. Schulhof, P. Heller, R. Nathans, and A. Linz, Phys. Rev. Lett. **24**, 1184 (1970).
[35] B. I. Halperin and P. C. Hohenberg, Phys. Rev. **188**, 898 (1969).
[36] D. L. Huber, Phys. Lett. **76A**, 406 (1980).
[37] H. J. M. de Groot and L. J. de Jongh, *Physics and Chemistry of Materials with Low-Dimensional Structures* (Ref. 31).
[38] A. Bienenstock, J. Appl. Phys. **37**, 1459 (1966).